New ligand substitution modes of $M_2(\mu\text{-}SR)_2(CO)_8$ (M = Mo, W; R = alkyl, aryl): synthesis, structure and properties of new di-nuclear metal(I) carbonyl thiolates, $[M_2(\mu\text{-}SPh)_2(CO)_xL_y]^{n-}$ (M = Mo, W; x = 6, 8; y = 0, 1; L = PhS, $(Ph)_2PCH_2P(Ph)_2$ and S_2CNEt_2; n = 1, 0) and a polymer $[W_2(\mu\text{-}SPh)_2(CO)_6(Ph)_2PCH_2P(Ph)_2]_m$

Botao Zhuang *, Haofen Sun, Guohua Pan, Lingjie He, Qiang Wei, Zhangfen Zhou, Saiqun Peng, Kechen Wu

State Key Laboratory of Structural Chemistry, Fujian Institute of Research on the Structure of Matter, Chinese Academy of Sciences, P.O. Box 143, Fuzhou, Fujian 350002, China

Abstract

Reaction of $[M_2(SC_6H_5)_2(CO)_8]$ (M = Mo, W) with NaSR (SR = SC_6H_5, S_2CNEt_2) in the presence of tetra-alkylammonium halide, or with diphenylphosphinemethane (DPPM = $(C_6H_5)_2P\,CH_2P\,(C_6H_5)_2$) in certain solvents affords new dinuclear metal(I)-carbonyl thiolates, $[W_2(SC_6H_5)_2(CO)_8]$ (**1**), $[Et_4N][Mo_2(SC_6H_5)_3(CO)_6]$ (**2**), $[Bu_4N][Mo_2(SC_6H_5)_2(CO)_6(S_2CNEt_2)]$ (**3**), $[W_2(SC_6H_5)_2(CO)_6DPPM]$ (**4**) and polymer $[W_2(SC_6H_5)_2(CO)_6 DPPM]_m$ (**5**). The crystal structures of **1**, **2**, **3** and **4** reveal that **1** contained a planar $[W_2S_2]$ unit, **2** had a $[Mo_2S_3]$ core with a planar Mo_2S_2 unit coordinated by a third SC_6H_5 bridging ligand and **3** and **4** possessed a planar $[M_2S_2]$ (M = Mo, W) core with two M atoms in different coordination environments. Three ligand substitution modes in the complexes were found: (i) substitution took place on the two M atoms in *cis*-direction resulting in three bridging ligand compound (for **2**); (ii) substitution occurred on one metal atom leading to unsymmetrical M_2S_2 unit (for **3** and **4**); and (iii) substitution occurred on the two M atoms in *trans*-direction to form a polymer (for **5**). IR, NMR and CV of these complexes were measured. An existence of mixed valence metal atoms leading to charge transfer and alteration of electrochemical behavior for the complexes were discussed and the possible structure of polymer compound **5** was proposed. © 2001 Published by Elsevier Science B.V.

Keywords: Substitution mode; Mo_2S_2-unit; W_2S_2 unit; Crystal structures; Spectroscopy and electrochemistry

1. Introduction

In 1984, thiolate ligands were reacted with $Mo(CO)_6$ (M = Mo, W) resulting in di-nuclear carbonyl complexes containing thiolate bridges, $[M_2(\mu\text{-}SR)_2(CO)_8]^{2-}$ (M = Mo, W; R = Ph, Bu^t) with a planar $[M_2S_2]$ core [1]. These carbonyl complexes undergo reversible two-electron oxidation accompanied by metal–metal bond

formation [2,3]. Decarbonylation of $[M_2(\mu\text{-}SR)_2(CO)_8]^{2-,0}$ and the subsequent reaction of its core $[M_2S_2]$ have attracted our attention because it may be useful for synthesizing a variety of multi-metal complexes that might contribute to understanding certain aspects of metal-enzymes. In order to investigate the reactivity of the $[M_2S_2]$ unit in the complexes, a series of ligand substituted dinuclear complexes such as the MeCN or PPh3-substituted compound, $[Mo_2(SPh)_2(CO)_6(MeCN)_2]$ and $[Mo_2(SPh)_2(CO)_6(PPh_3)_2]$ [4], acetate-substituted complexes, $[Mo_2(SPh)_2(CO)_6(RCOO)]^{-}$ [5,6], $[\{Mo_2(SPh)_2(CO)_6\}_2(OOCCH_2CH_2COO)_2]^{2-}$ [7],

* Corresponding author. Fax: + 86-591-3714946.
E-mail address: zbt@ms.fjirsm.ac.cn (B. Zhuang).

halide-substituted compounds, $[Mo_2(SPhCl)_2(CO)_6Br]^-$ [8], $[Mo_2(SPh)_2(CO)_6I]^-$ [9] and the DPPM substituted compound $[Mo_2(SPh)_2(CO)_6DPPM]^-$ [10] have been isolated and preliminarily investigated. The structure determinations indicate that there were three ligand substitution modes in these complexes. (i) The substitution may take place on the two M atoms with the substituting ligands on the different sides of the planar M_2S_2-unit, for example in MeCN-substituted compound, the so-called *trans*-substitution mode **A**; (ii) the substitution occurred on two metal atoms with the bidentate substituting ligand located at the same side of the planar M_2S_2-unit, as in acetate-substituted compounds, the so-called *cis*-substitution mode **B**; (iii) the substitution may occur on two M atoms by a monodentate bridging ligand, as in the halide-substituted compounds, the so-called bridge-forming substitution mode **C**. Recently we have obtained a thiolate-substituted Mo complex, $[Et_4N][Mo_2(SPh)_3(CO)_6]$ (**2**), as a new example of bridge-forming substitution mode **C**. Two other ligand-substituted Mo(W) thiolate carbonyl complexes, $[Bu_4N][Mo_2(SPh)_2(CO)_6(S_2CNEt_2)]$ (**3**) and $[W_2(SPh)_2(CO)_6(DPPM)]$ (**4**), have been discovered that adopt an unsymmetrical substitution mode **D** in which ligand-substitution has occurred on one M atom. Herein

A　　　**B**　　　**C**　　　**D**
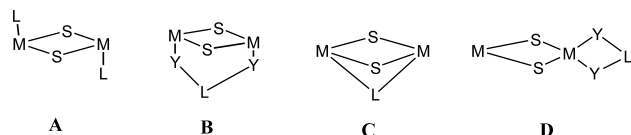
we report the synthesis, structure and spectroscopic characterization of new metal(I) thiolate carbonyl compounds: $[W_2(SPh)_2(CO)_8]$ (**1**), $[Et_4N][Mo_2(SPh)_3(CO)_6]$ (**2**), $[Bu_4N][Mo_2(SPh)_2(CO)_6(S_2CNEt_2)]$ (**3**), $[W_2(SPh)_2(CO)_6(DPPM)]$ (**4**) and $[W_2(SPh)_2(CO)_6(DPPM)]_m$ (**5**), and the possible structure of polymer complex $[W_2(SPh)_2(CO)_6(DPPM)]_m$ (**5**). Different substitution modes leading to change of configuration and differing electrochemical behavior of M_2S_2 unit in these complexes were also discussed.

2. Experimental

2.1. Materials and methods

All experiments were carried out under nitrogen atmosphere using standard Schlenk techniques and all solvents and reagents were dried and degassed before use. The compound $[Mo_2(SPh)_2(CO)_8]$ was prepared from $[Et_4N]_2[Mo_2(CO)_8(SR)_2]$ reacting with I_2 according to the literature methods [11]. IR spectra were recorded on a Nicolet-Magna 750 Fourier transform IR spectrometer or Digilab FTS-20E/D-V Fourier transform IR spectrometer. Elemental analysis was per-

formed on a CARLD ERBA instrumentation elemental analyzer MOD 1106; ^{13}C- and ^{95}Mo-NMR spectra were measured on a Varian-Unity-500 NMR spectrometer with a solution of 2 M Na_2MoO_4 in D_2O sealed in a capillary (for ^{95}Mo-NMR measurement) as reference. For comparison, the ^{13}C- and ^{95}Mo-NMR spectra of the compound $[Mo_2(SPh)_2(CO)_8]$ were also measured. Cyclic voltammetry (CV) measurements were performed with a three-electrode cell using 0.1 M Bu_4NBF_4 as the supporting electrolyte and acetone as solvent. The working electrode was glass carbon ($A = 0.0804$ cm^2), the reference electrode was an aqueous SCE separated from the sample solution by a salt bridge and the auxiliary electrode was platinum wire. Solutions were deoxygenated and blanketed with a nitrogen atmosphere and the potentiostat was a CV-B from BAS (Bioanalytical Systems).

2.2. Synthesis of $[W_2(SPh)_2(CO)_8]$ (**1**)

A mixture of $[Et_4N]_2[W_2(SR)_2(CO)_8]$ [12] (4.43 g, 4.1 mmol) and I_2 (1.05 g, 4.1 mmol) in 30 ml of CCl_4 was stirred at room temperature (r.t.) for 4 h. After filtering off the white residue, a dark green filtrate was concentrated to a volume of 5 ml by vacuum. To the concentrated filtrate was added 20 ml MeOH and 2.2 g of dark green micro-crystalline product $[W_2(SPh)_2(CO)_8]$ (**1**) which was obtained by filtration. The precipitate was washed with MeOH and dried in vacuum, yield 63%. Elemental Anal. Calc. for $C_{18}H_{10}O_8S_2W_2$: C, 29.6; H, 1.2; S, 7.9; W, 45.4. Found: C, 29.9; H, 1.6; S, 7.6; W, 46.2%. IR (KBr Pellet): 2031s, 1963s and 1939s cm^{-1} (v_{CO}).

2.3. Synthesis of $[Et_4N][Mo_2(SPh)_3(CO)_6]$ (**2**)

A mixture of 0.08 g (0.61 mmol) NaSPh and 0.12 g (0.72 mmol) Et_4NCl in MeCN was stirred at 40 °C overnight, then filtered. To the filtrate was added 0.3 g (0.47 mmol) $[Mo_2(SPh)_2(CO)_8]$, and the resulting mixture was stirred at 40 °C for another 24 h resulting in red brown solution. This red brown solution was concentrated to 10 ml under vacuum, and then 20 ml MeOH was added. After cooling to 4 °C overnight, 0.24 g (0.29 mmol) of black microcrystalline **2** was obtained by filtration. The product was washed with MeOH and dried under vacuum. Yield, 48% (based on the amount of NaSPh used). Anal. Calc. for $C_{32}H_{35}Mo_2NO_6S_3$: C, 47.0; H, 4.3; N, 1.7; S, 11.7. Found: C, 47.1; H, 4.3; N, 1.8; S, 11.5%. IR (KBr pellet): 1998m, 1965s, 1940s, 1917s, 1849s cm^{-1} (v_{MoC-O}), 608m, 579m, 507m, 498m cm^{-1} (δ_{Mo-C-O}), 370w, 351m (v_{Mo-C}) and 433sh, 419m cm^{-1} (v_{Mo-S}). The single crystals suitable for X-ray crystallography were grown from the mixed solvents of MeCN/MeOH.

2.4. Synthesis of [Bu$_4$N][Mo$_2$(SPh)$_2$(CO)$_6$(S$_2$CNEt$_2$)] (3)

1. 0.634 g (1 mmol) of [Mo$_2$(SPh)$_2$(CO)$_8$] were dissolved in 20 ml of acetone resulting in dark green solution, after which 0.322 g (1 mmol) Bu$_4$NBr was added. The resulting solution was stirred at 50 °C for half an hour then cooled to r.t. After adding 0.17 g (1 mmol) of NaS$_2$CNEt$_2$, the reaction mixture was stirred at r.t. for 12 h and the resulting red–brown solution was reduced to 10 ml under vacuum and filtered. To the filtrate was added 20 ml of isopropanol. After filtering off a small amount of residue and cooling at 4 °C for several days, 0.5 g of dark brown micro-crystalline product, [Bu$_4$N]-[Mo$_2$(SPh)$_2$(CO)$_6$(S$_2$CNEt$_2$)] (3), was obtained by filtration, washed with isopropanol and dried in vacuum, yield, 52%. Elemental Anal. Calc. for C$_{59}$H$_{56}$N$_2$Mo$_2$O$_6$S$_4$: C, 48.4; H, 5.8; N, 2.9. Found: C, 48.3; H, 5.9; N, 2.9%. IR (KBr pellet): 2017s, 1928s, 1898s and 1799s (ν_{MoC-O}).
2. To a solution of [Bu$_4$N][Mo$_2$(SPh)$_2$(CO)$_6$Br] [9] (0.4 g, 0.5 mmol) in acetone (20 ml) was added 0.085g (0.5 mmol) of NaS$_2$CNEt$_2$. The resulting mixture was stirred at 50 °C for half an hour and at r.t. for another 12 h. The red–brown solution was concentrated to 10 ml and then filtered. To the filtrate was added 20 ml of isopropanol. After filtering off a small amount of precipitate and cooling at 4 °C for several days, a dark brown micro-crystalline product was collected, which was recognized as 3 by its IR spectrum.

2.5. Synthesis of [W$_2$(SPh)$_2$(CO)$_6$DPPM] (4)

A mixture of 0.40 g (0.5 mmol) of [W$_2$(SPh)$_2$(CO)$_8$] (1) and 0.19 g (0.5 mmol) of DPPM in 20 ml of toluene was stirred at r.t. for 24 h resulting in green brown solution. The resulting solution was concentrated to 10 ml by vacuum and 20 ml of methanol was added. 0.95 g of green product [W$_2$(SPh)$_2$(CO)$_6$DPPM] (4)·1/2 C$_7$H$_8$ was obtained by filtration, washed with MeOH and dried in vacuum. Yield: 81.4%. Elemental Anal. Calc. for C$_{43}$H$_{32}$O$_6$P$_2$S$_2$·1/2 C$_7$H$_8$: C, 47.1; H, 3.0; P, 5.2; S, 5.4. Found: C, 47.2; H, 3.2; P, 5.0; S, 5.5%. IR (KBr pellet): 2033(m), 1956(s), 1925(s) and 1840(m) cm^{-1}.

2.6. Synthesis of polymer [W$_2$(SPh)$_2$(CO)$_6$DPPM]$_m$ (5)

A mixture of 0.40 g (0.5 mmol) of [W$_2$(SPh)$_2$(CO)$_8$] and 0.38 g (1.0 mmol) of DPPM in 25 ml of toluene was stirred at r.t. for 24 h affording a dark green precipitate. The dark green solid product 5 was isolated by filtration, washed with toluene and dried in vacuum. Yield: 0.45 g. IR (KBr pellet): 2006(w), 1979(s), 1927(s), 1896(s) and some characteristic absorption of DPPM ligand. Elemental Anal.: C, 52.1; H, 3.6; P, 6.0; S, 6.1; W, 35.8% showed that the atom ratio was C:H:P:S:W: ≈ 43:32:2:2:2. Product 5 is almost insoluble in CCl$_4$, MeCN, benzene, toluene, acetone and methanol, and is slightly soluble in CH$_2$Cl$_2$, Me$_2$SO, cyclohexane and hexane.

2.7. X-ray crystal structure determination

The crystal data and experimental conditions are given in Table 1. All the samples were mounted on the glass fiber and coated with epoxy cement. The intensities of 1, 2 and 4·1/2 C$_7$H$_8$ were collected on an Enraf-Nonius CAD4 computer controlled kappa axis diffractometer. A total of 2513 (for 1), 3454 (for 2) and 7734 (for 4·1/2 C$_7$H$_8$) were collected. Lorentz and polarization corrections were applied to the data. An empirical absorption correction (base on a series of psi-scans) was applied to the data. Relative transmission coefficients ranged from 0.663 to 0.998 (for 1), 0.949 to 1.000 (for 2) and 0.654 to 0.999 (for 4·1/2 C$_7$H$_8$). The structures of 1 and 2 were solved by direct methods with MOLTAN-83 program. A total of two atoms were located from an E-map prepared from the phase set with probability statistics: absolute figure of merit = 1.04 (for 1), 1.02 (for 2) and residual = 5.82 (for 1), 8.67 (for 2). The structure of 4·1/2 C$_7$H$_8$ was solved using Patterson heavy-atom method which revealed the heavy atoms. The remaining atoms were located in succeeding difference Fourier syntheses. Hydrogen atoms were located and added to the structure factor calculations but their positions were not refined. The structures were refined using full-matrix least-squares where the function minimized was $\Sigma\, w(|F_o| - |F_c|)^2$ and the weight w is defined as $w = F_o/43.27$ if $F_o < 43.27$ or $w = 43.27/F_o$ if $F_o \geq 43.27$ and $w = w^2$ if $w \geq 0.10$, $w = 0.0$ if $w < 0.10$ (for 1); and as per the Killean and Lawrence method with terms of 0.010 and 1.0 [13] (for 1 and 4·1/2 C$_7$H$_8$). The final cycle of refinement converged with unweighted and weighted agreement factors of $R_1 = \Sigma\, ||F_o| - |F_c||/\Sigma\, |F_o|$ and $R_w = [\Sigma\, w(F_o - F_c)^2/\Sigma\, wF_o^2]^{1/2}$. All the calculations were performed by using MolEN/PC [14]. The data collection of 3 was performed on a Siemens Smart CCD diffractometer with graphite–monochromatic Mo–K$_\alpha$ radiation. A total of 9146 refractions were collected and the data reductions were performed on a silicon graphics computer station with SMART CCC software. The structure of 3 was solved by conventional direct methods (SHELXTL) and was refined by the full-matrix least-squares method on F^2 data using a Silicon Graphics INDY computer and local programs [15]. All non-hydrogen atoms were refined anisotropically; hydrogen atoms were located at idealized positions and refined with fixed isotropic thermal parameters. The final refinement converged with unweighted and weighted agreement

factors of $R_1 = \Sigma \, ||F_o| - |F_c||/\Sigma \, |F_o|$ and $wR_2 = [\Sigma \, w(F_o^2 - F_c^2)^2/\Sigma \, w(F_o^2)^2]^{1/2}$.

3. Results and discussion

3.1. Synthesis of the complexes and ligand substitution reaction

The complex $[W_2(SPh)_2(CO)_8]$ (**1**) was prepared as the Mo-analog $[Mo_2(SPh)_2(CO)_8]$ [11] according to reaction (Eq. (1)):

$$[Et_4N]_2[W_2(SPh)_2(CO)_8] + I_2 \xrightarrow{CCl_4} [W_2(SPh)_2(CO)_8]$$
$$+ 2[Et_4N]I \qquad (1)$$
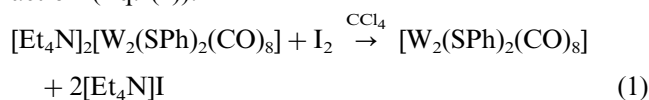
In Eq. (1), $[Et_4N]_2[W_2(SPh)_2(CO)_8]$ (no W–W bond) underwent two-electron oxidation by I_2 affording complex **1** with creation of W–W bond. The choice of solvents is very important, non-coordinating solvents such as CCl_4, toluene or hexane are suitable for preparing complex **1** in high yield. Coordinating solvents such as MeCN, DMF and DMSO lead to the formation of solvent substituted compounds (Eq. (2)).

$$[M_2(SPh)_2(CO)_8]^{2-} + I_2$$
$$\xrightarrow{Solvent} [M_2(SPh)_2(CO)_6(Solvent)_2] + 2I^- + 2CO \qquad (2)$$
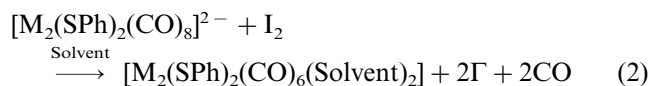
The metal(I)-complex $[Mo_2(SPh)_2(CO)_8]$ [11] reacted with thiolate ligand PhS^- resulting in a triply bridged dinuclear Mo(I)-complex which was isolated as a tetraethylammonium salt, $[Et_4N][Mo_2(SPh)_3(CO)_8]$ (**2**). This substitution reaction (Eq. (3)), like the reaction of halide substituted complexes [8,9], adopts the bridge-forming substitution mode **C**.

$$[Mo_2(SPh)_2(CO)_8] + [Et_4N]SPh \xrightarrow{MeCN} [Et_4N]$$
$$[Mo_2(SPh)_3(CO)_6] + 2CO \qquad (3)$$
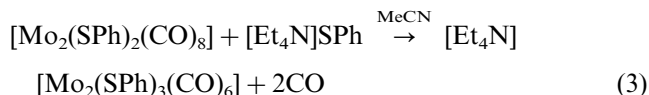
In contrast to ^-SPh, $^-S_2CNEt_2$, reacted with $[Mo_2(SPh)_2(CO)_8]$ in the presence of Bu_4NBr affording $[Bu_4N][Mo_2(SPh)_2(S_2CNEt_2)]$ (**3**), in which the $^-S_2CNEt_2$ ligand chelates one Mo atom leading to an unsymmetrical Mo_2S_2 core in the molecule (Eq. (4)). In this case, the reaction adopted a new substitution mode giving unsymmetrical geometry **D**.

$$[Mo_2(SPh)_2(CO)_8] + NaS_2CNEt_2$$
$$\xrightarrow[-NaBr]{Bu_4NBr} [Bu_4N][Mo_2(SPh)_2(CO)_6S_2CNEt_2] + 2CO \qquad (4)$$
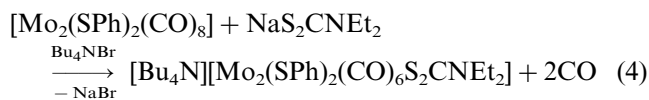
Reaction of $[W_2(SPh)_2(CO)_8]$ (**1**) with DPPM unexpectedly formed an unsymmetrical substitution mode **D** product, $[W_2(SPh)_2(CO)_6DPPM]$ (**4**), in contrast with the Mo-analog, $[Mo_2(SPh)_2(CO)_6DPPM]$, which is a

Table 1
Crystallographic data and data collection parameters for complexes **1**, **2**, **3** and **4**·1/2 C_7H_8

Compounds	**1**	**2**	**3**	**4**·1/2 C_7H_8
Empirical formula	$C_{20}H_{10}O_8S_2W_2$	$C_{32}H_{35}Mo_2NO_6S_3$	$C_{39}H_{56}Mo_2N_2O_6S_4$	$C_{46.5}H_{36}O_6P_2S_2W_2$
Formula weight	810.13	817.17	968.98	1184.58
Crystal system	Monoclinic	Monoclinic	Triclinic	Triclinic
Space group	$P2_1/c$	C_C	$P-1$	$P-1$
Unit cell dimensions				
a (Å)	9.172(2)	19.951(4)	11.1489(4)	11.108(2)
b (Å)	12.045(2)	11.046(2)	12.4039(4)	12.195(6)
c (Å)	11.152(2)	17.721(2)	19.4625(4)	16.247(9)
α (°)			103.6410(10)	101.83(5)
β (°)	111.58(2)	112.45(4)	96.542(2)	85.03(2)
γ (°)			114.1470(10)	95.91(2)
V (Å³)	1146	3609	2319	2204
Z	2	4	2	2
D_{calc} (g cm⁻³)	1.35	1.50	1.39	1.79
$F(000)$	748	1656	1000	1146
$\mu(Mo-K_\alpha)$ (cm⁻¹)	140.7	8.8	7.63	55.4
Diffractometer	Enraf-Nonius CAD4	Enraf-Nonius CAD4	Siemens Smart CCD	Enraf-Nonius CAD4
Temperature (°C)	23 ± 1	23 ± 1	23 ± 1	23 ± 1
Radiation	Mo–K$_\alpha$ (0.71073 Å)	Mo–K$_\alpha$ (0.71073 Å)	Mo–K$_\alpha$ (0.71073 Å)	Mo–K$_\alpha$ (0.71073 Å)
Scan type	$\omega-\theta$	$\omega-\theta$	$\omega-\theta$	$\omega-\theta$
$2\theta_{max}$ (°)	52.0	50.0	46.6	50.0
No. of observations [$I > 3.0\sigma(I)$]	2026	2878	6482 ($F^0 > 4.0\sigma(F)$)	5093
No. of variables (p)	145	440	478	524
R	0.032	0.035	0.064	0.053
R_w (or wR_2)	0.033	0.036	0.1455(wR_2)	0.064
Goodness-of-fit	0.82	0.69	0.833	0.50
Maximum shift in final cycle	0.01σ	0.48σ	0.98σ	0.02σ
Largest peaks in final difference map (e Å⁻³)	1.52(47)	0.40(6)	0.817	1.73(22)

$$[M_2(CO)_8(SPh)_2]$$
(M=Mo or W)
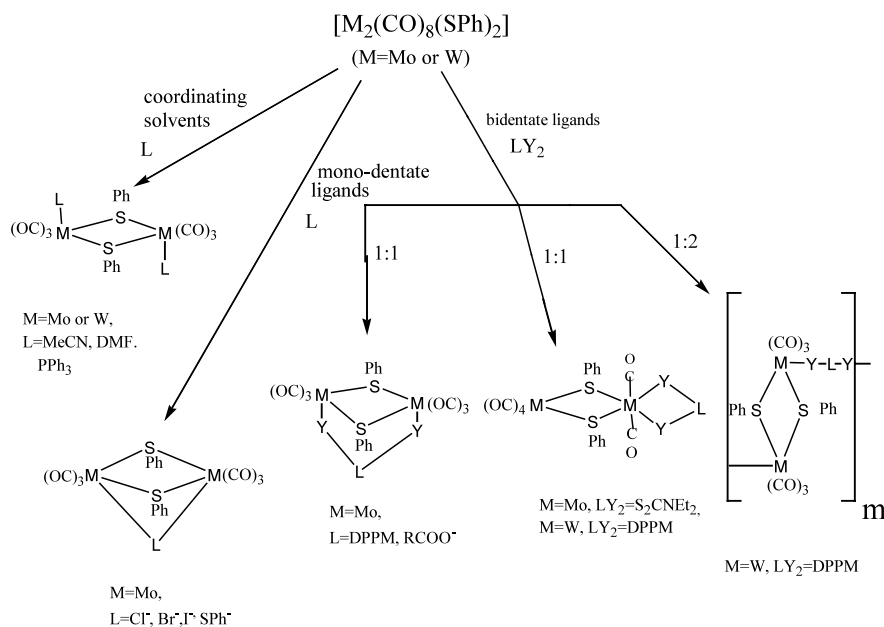
Scheme 1.

cis-substitution mode **B** product [10]. It is worth point- ing out that if the ratio of [W₂(SPh)₂(CO)₈]:DPPM is 1:2, a less soluble DPPM-containing W–S–CO polymer (**5**), which possesses an IR spectrum very different from complex **4**, is obtained in high yield.

So far the ligand substitution reactions of [M₂(SPh)₂(CO)₈] (M = Mo, W) can be summarized as following Scheme 1.

It is worth pointing out that the axial M–CO bond distances are longer than the equatorial ones in the structure of [M₂(CO)₈(SPh)₂] (M = Mo, W). This may imply that the axial carbonyls are easier to substitute than the equatorial carbonyls. Therefore, in the ligand substitution reaction, the ligands always replace the axial carbonyls first. In some cases, if the ligands have large steric bulk, the replacement occurs at the equato- rial position. For instance, complex **4**, owing to the larger stereo-hindrance of DPPM than the S₂CNEt₂ ligand in complex **3**, undergoes substitution at equato- rial positions, and complex **3** adopted substitution at both axial and equatorial positions simultaneously (see next section).

Interestingly, the reaction of [Mo₂(SPh)₂(CO)₆Br]⁻ with S₂CNEt₂⁻ ligand did not result in *cis*-substitution mode **B** product [Mo₂(CO)₆(μ-SPh)₂(μ-S₂CNEt₂)]⁻ but rather in the unsymmetrical substitution mode **D** product, complex **3**. The two phenyl rings of SPh⁻ ligands in **3** are *trans*-relative to the Mo₂S₂ plane in contrast with [Mo₂(SPh)₂(CO)₆Br]⁻ in which the two phenyl rings are *cis* [8]. This means that the reaction is not a simple substitution of Br bridge by S₂CNEt₂⁻, but involves dissociation of the Br⁻ bridge, a change of the arrangement of phenyl rings and coordination of

S₂CNEt₂ ligand. It is evident that according to its elemental analysis data, IR spectrum and solubility, **5** is different from **4** and might be a polymer of *trans*-sub- stitution mode **A** product [4]. The acquirement of poly- mer **5** is significant because it makes possible to connect M₂S₂ units in different arrangements by using special multi-dentate ligands.

3.2. Structures of *1*, *2*, *3*, *4* and possible structure of polymer *5*

The selected bond distances and angles of **1**, **2**, **3** and **4** are listed in Tables 2–5, respectively, and the struc- tures of **1**, **2**, **3** and **4** are depicted in Figs. 1–4, respectively.

All four complexes possess a planar M₂S₂-unit (M = Mo or W) with small change of dimensions shown in Table 6.

The structure of **1** (Fig. 1) is centro-symmetric with the geometry around each W atom being a distorted octahedron with four carbon atoms from carbonyls and two sulfur atoms from two bridging SPh ligands. The geometry of the W₂S₂ core is almost the same as that of Mo₂S₂ unit in the Mo-analog, [Mo₂(SPh)₂(CO)₈] [11].

Complex **2** is comprised of a cation Et₄N⁺ and a di-nuclear molybdenum anion with three thiolate bridges, [Mo₂(SPh)₃(CO)₆]⁻. As shown in Fig. 2, the structure of the anion of **2** contains a [Mo₂S₃] core (E) with a planar Mo₂S₂ unit. As is listed in Table 6, the dimension of the Mo₂S₂ unit in **2** is contracted by 0.01 Å of Mo–S, 0.08 Å of Mo–Mo and 2.23° of Mo–S–Mo than that in [Mo₂(SPh)₂(CO)₈], and the Mo₂S₂ unit of **2** was slightly puckered with dihedral angle of 12.17° between Mo(1)–Mo(2)–S(1) and

Mo(1)–Mo(2)–S(2) due to the introduction of the third SPh bridge. For the third bridge, the Mo–S bond distance is 2.592(3) Å and Mo–S–Mo angle is 67.66°. Around the [Mo$_2$S$_3$] core, there are three carbonyls coordinated to each Mo^I atom and one phenyl group linking to each sulfur atom. Two phenyl groups on the S atoms of Mo$_2$S$_2$ plane are on the same side of the M$_2$S$_2$ plane resulting in *syn*-configuration which is different from the *anti*-configuration in Mo$_2$(SPh)$_2$(CO)$_8$. The structure of the anion of **2** could be described as face-shared bi-octahedron (**F**).
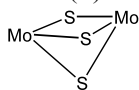
E

It is worth noting that the axial Mo–C (1.92 Å) is shorter than the equatorial Mo–C (1.97 Å) in complex **2**, and both the axial and equatorial Mo–C distances in **2** are shorter than that in Mo$_2$(SPh)$_2$(CO)$_8$ (2.05 and 2.02 Å). This means that the carbonyls of **2** are more difficult to be further substituted. In fact, quartet bridge-compound or the other product resulted from further substitution of carbonyls of **2** are not isolated, at least in this reaction system, so far.
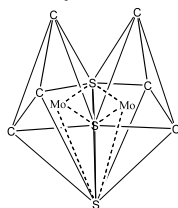
F

Table 2
Selected bond lengths (Å) and bond angles (°) for [W$_2$(SPh)$_2$(CO)$_8$] (**1**)

Bond lengths			
W(1)–W(1′)	2.9691(7)	W(1)–C(4)	2.03(2)
W(1)–S(1)	2.477(2)	S(1)–C(11)	1.808(9)
W(1)–S(1′)	2.476(2)	O(1)–C(1)	1.15(1)
W(1)–C(1)	2.02(2)	O(2)–C(2)	1.14(1)
W(1)–C(2)	2.00(1)	O(3)–C(3)	1.13(1)
W(1)–C(3)	2.06(1)	O(4)–C(4)	1.12(1)
Bond angles			
W(1)–W(1′)–S(1)	53.15(6)	C(1)–W(1)–C(2)	84.2(4)
W(1′)–W(1)–S(1)	53.20(5)	C(1)–W(1)–C(3)	173.9(5)
W(1′)–W(1)–C(1)	94.5(3)	C(1)–W(1)–C(4)	91.0(4)
W(1′)–W(1)–C(2)	137.5(3)	C(2)–W(1)–C(3)	95.7(4)
W(1′)–W(1)–C(3)	89.7(3)	C(2)–W(1)–C(4)	84.9(4)
W(1′)–W(1)–C(4)	137.5(3)	C(3)–W(1)–C(4)	82.9(4)
S(1)–W(1)–S(1′)	106.34(6)	W(1)–S(1)–W(1′)	73.66(6)
S(1)–W(1)–C(1)	85.7(3)	W(1)–S(1)–C(11)	117.6(3)
S(1)–W(1)–C(2)	103.1(3)	W(1′)–S(1)–C(11)	113.3(4)
S(1)–W(1)–C(3)	82.9(3)	W(1)–C(1)–O(1)	175(1)
S(1)–W(1)–C(4)	162.1(3)	W(1)–C(2)–O(2)	175(2)
S(1′)–W(1)–C(1)	82.3(3)	W(1)–C(3)–O(3)	176.8(9)
S(1′)–W(1)–C(2)	163.7(3)	W(1)–C(4)–O(4)	179(2)
S(1′)–W(1)–C(3)	96.7(3)	S(1)–C(11)–C(12)	124.5(8)
S(1′)–W(1)–C(4)	86.1(3)	S(1)–C(11)–C(16)	116.1(9)

Table 3
Selected bond lengths (Å) and bond angles (°) of [Et$_4$N][Mo$_3$(CO)$_6$-(SPh)$_3$] (**2**)

Bond lengths			
Mo(1)–Mo(2)	2.877(2)	Mo(2)–C(5)	1.91(2)
Mo(1)–S(1)	2.462(3)	Mo(2)–C(6)	1.97(1)
Mo(1)–S(2)	2.462(3)	S(1)–C(11)	1.77(2)
Mo(1)–S(3)	2.576(3)	S(2)–C(21)	1.778(9)
Mo(1)–C(1)	1.95(1)	S(3)–C(31)	1.76(2)
Mo(1)–C(2)	1.93(2)	O(1)–C(1)	1.16(1)
Mo(1)–C(3)	1.97(1)	O(2)–C(2)	1.15(1)
Mo(2)–S(1)	2.470(4)	O(3)–C(3)	1.17(1)
Mo(2)–S(2)	2.476(3)	O(4)–C(4)	1.15(1)
Mo(2)–S(3)	2.592(3)	O(5)–C(5)	1.16(2)
Mo(2)–C(4)	1.97(1)	O(6)–C(6)	1.16(1)
Bond angles			
Mo(2)–Mo(1)–S(1)	54.45(7)	Mo(1)–Mo(2)–S(1)	54.17(7)
Mo(2)–Mo(1)–S(2)	54.49(7)	Mo(1)–Mo(2)–S(2)	54.14(6)
Mo(2)–Mo(1)–S(3)	56.44(7)	Mo(1)–Mo(2)–S(3)	55.91(7)
Mo(2)–Mo(1)–C(1)	136.2(4)	Mo(1)–Mo(2)–C(4)	136.2(4)
Mo(2)–Mo(1)–C(2)	106.8(3)	Mo(1)–Mo(2)–C(5)	108.6(4)
Mo(2)–Mo(1)–C(3)	135.3(3)	Mo(1)–Mo(2)–C(6)	135.7(4)
S(1)–Mo(1)–S(2)	108.1(2)	S(1)–Mo(2)–S(2)	107.4(1)
S(1)–Mo(1)–S(3)	77.71(9)	S(1)–Mo(2)–S(3)	77.25(9)
S(1)–Mo(1)–C(1)	166.8(4)	S(1)–Mo(2)–C(4)	166.8(4)
S(1)–Mo(1)–C(2)	95.0(4)	S(1)–Mo(2)–C(5)	95.5(4)
S(1)–Mo(1)–C(3)	84.7(3)	S(1)–Mo(2)–C(6)	85.0(4)
S(2)–Mo(1)–S(3)	73.42(9)	S(2)–Mo(2)–S(3)	72.9(1)
S(2)–Mo(1)–C(1)	84.1(4)	S(2)–Mo(2)–C(4)	84.6(4)
S(2)–Mo(1)–C(2)	94.8(3)	S(2)–Mo(2)–C(5)	96.6(3)
S(2)–Mo(1)–C(3)	164.4(3)	Mo(1)–C(1)–O(1)	178(1)
S(3)–Mo(1)–C(1)	102.0(4)	Mo(1)–C(2)–O(2)	177.7(9)
S(3)–Mo(1)–C(2)	163.0(3)	Mo(1)–C(3)–O(3)	175(2)
S(3)–Mo(1)–C(3)	101.8(4)	Mo(2)–C(4)–O(4)	179(1)
C(1)–Mo(1)–C(2)	88.6(5)	Mo(2)–C5–O5	177.2(9)
C(1)–Mo(1)–C3	82.5(5)	Mo(2)–C6–O6	177(1)
C(2)–Mo(1)–C3	92.6(5)	S(1)–C(11)–C(12)	120.7(9)

Complex **3** consists of a cation [Bu$_4$N]$^+$ and an anion [(OC)$_4$Mo(SPh)$_2$Mo(CO)$_2$(S$_2$CNEt$_2$)]$^-$. As shown in Fig. 3, the structure of the anion of **3** possesses an unsymmetrical rhombic core [Mo$_2$S$_2$] with two different Mo–S distances (average Mo(1)–S of 2.41 Å and Mo(2)–S of 2.55 Å). Around the core, there are four carbonyls coordinated to one Mo atom and two carbonyls and one dithiocarbamate ligand S$_2$CNEt$_2$ coordinated to another Mo atom forming different coordination environments of the two Mo atoms. The whole geometry could be considered as an egde-shared bi-octahedron (**G**). Two phenyl-rings link to the sulfur atoms in *anti*-configuration relative to the Mo$_2$S$_2$ plane. In terms of the different values of Mo(1)–S(Ph) and Mo(2)–S(Ph) bond distances in **3** and consulting the Mo(I)-complexes [Mo$_2$(SPh)$_2$(CO)$_8$] (Mo–S, 2.474 Å) and Mo(0)-complex, [Mo$_2$(SPh)$_2$(CO)$_8$]$^{2-}$ (Mo–S, 2.608 Å), the two Mo atoms in compound **3** are obviously in different oxidation states and the oxidation state of the Mo(2) with four carbonyl ligands is between +1 and 0, and the valence of the Mo(1) atom with S$_2$CNEt$_2$

ligand is higher than +1. This indicates that the un-symmetric substitution mode resulting from the introduction of dithiocarbamate ligand leads to a Mo(1) → Mo(2) charge transfer and formation of a mixed valence complex. The S_2CNEt_2 ligand replaces one axial carbonyl and one equatorial carbonyl on a Mo atom in **3** rather than bridges two Mo atoms. The S_2CNEt_2 ligand in **3** is evidently a conjugate system in terms of the C–N of 1.34 Å (between single and double bonds), CNC of ca. 120°, SCN of 122° and SCS of 114°.
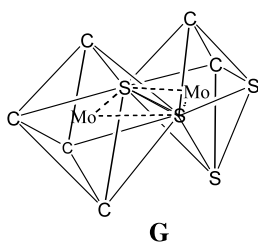
G

The complex **4**, $[W_2(SPh)_2(CO)_6(DPPM)]$, also contains an unsymmetrical rhombic W_2S_2 unit with W(1)–S

of 2.55 Å, W(2)–S of 2.43 Å and W(1)–W(2) of 2.996 Å (Table 6). The whole structure of **4** is similar to that of the anion of complex **3** except for the different coordination positions of DPPM and S_2CNEt_2. The DPPM coordinates to two equatorial positions of one W atom in **4** (Fig. 4) and the S_2CNEt_2 coordinates to one axial and one equatorial positions of one Mo atom in **3** (Fig. 3). This is obviously due to the larger steric demand of DPPM compared to S_2CNEt_2. DPPM not only can coordinate to two equatorial positions of one metal atom but also can bridge two metal atoms in axial positions if the steric hindrance could be effectively reduced in the final product. In fact, the Mo compound with DPPM bridge, $[Mo_2(\mu-SPh)_2(CO)_6(\mu-DPPM)]$, in which the phenyl rings are in *syn*-arrangement relative to Mo_2S_2 unit plane, have been isolated [10]. In examining the W–S bond distances of W(0)-complex, $[W_2(SCH_2CO_2Me)_2(CO)_8]^{2-}$ (2.58 Å) [16], $[W_2(SPh)_2(CO)_8]^{2-}$ (2.59 Å) [17] and W(I)-complex **1** (2.47 Å), it can be found that, similar to complex **3**, the oxidation state of W(2) attached to the DPPM ligand (> +1) is higher than the valence of W_1 with four

Table 4
Selected bond lengths (Å) and bond angles (°) of **3**

Bond lengths

Mo(1)–C(2)	1.921(9)	Mo(2)–C(6)	2.023(9)	C(01)–C(02)	1.479(13)
Mo(1)–C(1)	1.990(11)	Mo(2)–S(1)	2.552(2)	C(03)–C(04)	1.492(12)
Mo(1)–S(1)	2.362(2)	Mo(2)–S(2)	2.554(2)	C(1)–O(1)	1.158(10)
Mo(1)–S(2)	2.451(2)	S(1)–C(11)	1.791(8)	C(2)–O(2)	1.171(9)
Mo(1)–S(11)	2.488(2)	S(2)–C(21)	1.794(8)	C(3)–O(3)	1.154(11)
Mo(1)–S(12)	2.592(4)	S(11)–C(0)	1.715(8)	C(4)–O(4)	1.132(10)
Mo(1)–Mo(2)	3.0396(10)	S(12)–C(0)	1.699(8)	C(5)–O(5)	1.135(10)
Mo(2)–C(3)	1.952(13)	N(0)–C(0)	1.340(9)	C(6)–O(6)	1.149(9)
Mo(2)–C(5)	1.981(11)	N(0)–C(03)	1.463(10)		
Mo(2)–C(4)	2.016(10)	N(0)–C(01)	1.499(10)		

Bond angles

C(2)–Mo(1)–C(1)	78.5(4)	C(5)–Mo(2)–C(4)	87.9(4)	C(21)–S(2)–Mo(2)	119.1(3)
C(2)–Mo(1)–S(1)	103.1(2)	C(3)–Mo(2)–C(6)	89.9(4)	Mo(1)–S(2)–Mo(2)	74.75(6)
C(1)–Mo(1)–S(1)	89.5(3)	C(5)–Mo(2)–C(6)	86.0(4)	C(0)–S(11)–Mo(1)	90.1(3)
C(2)–Mo(1)–S(2)	84.4(2)	C(4)–Mo(2)–C(6)	173.9(4)	C(0)–S(12)–Mo(1)	86.9(3)
C(1)–Mo(1)–S(2)	157.5(3)	C(3)–Mo(2)–S(1)	172.8(4)	C(0)–N(0)–C(03)	121.5(7)
S(1)–Mo(1)–S(2)	108.64(8)	C(5)–Mo(2)–S(1)	85.6(3)	C(0)–N(0)–C(01)	120.4(7)
C(2)–Mo(1)–S(11)	104.5(3)	C(4)–Mo(2)–S(1)	95.6(3)	C(03)–N(0)–C(03)	118.2(7)
C(1)–Mo(1)–C(11)	81.1(3)	C(6)–Mo(2)–S(1)	84.8(3)	N(0)–C(0)–S(12)	124.1(6)
S(1)–Mo(1)–S(11)	148.33(8)	C(3)–Mo(2)–S(2)	85.6(3)	N(0)–C(0)–S(11)	121.7(6)
S(2)–Mo(1)–S(11)	89.33(8)	C(5)–Mo(2)–S(2)	172.7(3)	S(12)–C(0)–S(11)	114.2(5)
C(2)–Mo(1)–S(12)	172.7(2)	C(4)–Mo(2)–S(2)	86.8(3)	C(02)–C(01)–N(0)	110.9(9)
C(1)–Mo(1)–S(12)	102.4(3)	C(6)–Mo(2)–S(2)	99.2(2)	N(0)–C(03)–C(04)	112.7(8)
S(1)–Mo(1)–S(12)	84.21(7)	S(1)–Mo(2)–S(2)	99.95(7)	O(1)–C(1)–Mo(1)	174.9(9)
S(2)–Mo(1)–S(12)	92.84(7)	C(3)–Mo(2)–Mo(1)	136.7(3)	O(2)–C(2)–Mo(1)	176.7(8)
S(11)–Mo(1)–S(12)	68.64(7)	C(5)–Mo(2)–Mo(1)	133.8(3)	O(3)–C(3)–Mo(2)	178.2(10)
C(2)–Mo(1)–Mo(2)	92.6(3)	C(4)–Mo(2)–Mo(1)	88.7(3)	O(4)–C(4)–Mo(2)	175.5(11)
C(1)–Mo(1)–Mo(2)	104.4(3)	C(6)–Mo(2)–Mo(1)	96.1(2)	O(5)–C(5)–Mo(2)	175.5(10)
S(1)–Mo(1)–Mo(2)	54.65(6)	S(1)–Mo(2)–Mo(1)	49.02(5)	O(6)–C(6)–Mo(2)	171.3(8)
S(2)–Mo(1)–Mo(2)	54.16(6)	S(2)–Mo(2)–Mo(1)	51.09(5)	C(16)–C(11)–S(1)	125.3(7)
S(11)–Mo(1)–Mo(2)	138.15(6)	C(11)–S(1)–Mo(1)	119.8(3)	C(12)–C(11)–S(1)	115.5(7)
S(12)–Mo(1)–Mo(2)	91.23(5)	C(11)–S(1)–Mo(2)	112.9(3)	C(22)–C(21)–S(2)	125.3(6)
C(3)–Mo(2)–C(5)	89.3(4)	Mo(1)–S(1)–Mo(2)	76.33(6)	C(26)–C(21)–S(2)	114.9(6)
C(3)–Mo(2)–C(4)	89.2(4)	C(21)–S(2)–Mo(1)	114.5(3)		

Table 5
Selected bond lengths (Å) and bond angles (°) of [W$_2$(SPh)$_2$(CO)$_6$(DPPM)] (**4**)

Bond lengths					
W(1)–W(2)	2.996(2)	W(2)–P(1)	2.489(4)	P(2)–C	1.86(2)
W(1)–S(1)	2.541(5)	W(2)–P(2)	2.488(4)	P(2)–C(51)	1.92(2)
W(1)–S(2)	2.556(5)	W(2)–C(5)	2.03(2)	P(2)–C(61)	1.81(2)
W(1)–C(1)	1.96(2)	W(2)–C(6)	1.98(2)	O(1)–C(1)	1.16(2)
W(1)–C(2)	1.98(2)	S(1)–C(11)	1.76(2)	O(2)–C(2)	1.14(2)
W(1)–C(3)	2.00(2)	S(2)–C(21)	1.78(2)	O(3)–C(3)	1.15(2)
W(1)–C(4)	2.06(3)	P(1)–C	1.85(2)	O(4)–C(4)	1.11(2)
W(2)–S(1)	2.437(4)	P(1)–C(31)	1.83(2)	O(5)–C(5)	1.14(2)
W(2)–S(2)	2.431(4)	P(1)–C(41)	1.79(2)	O(6)–C(6)	1.17(2)
Bond angles					
W(2)–W(1)–S(1)	51.4(2)	S(1)–W(2)–S(2)	109.6(2)	W(2)–P(2)–C	97.3(7)
W(2)–W(1)–S(2)	52.2(1)	S(1)–W(2)–P(1)	159.5(5)	W(2)–P(2)–C(51)	122.0(5)
W(2)–W(1)–C(1)	134.3(6)	S(1)–W(2)–P(2)	91.7(2)	W(2)–P(2)–C(61)	117.7(7)
W(2)–W(1)–C(2)	135.6(5)	S(1)–W(2)–C(5)	85.4(5)	C–P(2)–C(51)	104.7(9)
W(2)–W(1)–C(3)	93.2(7)	S(1)–W(2)–C(6)	97.3(6)	C–P(2)–C(61)	108.2(9)
W(2)–W(1)–C(4)	90.4(6)	S(2)–W(2)–P(1)	90.9(1)	C(51)–P(2)–C(61)	105.1(7)
S(1)–W(1)–S(2)	102.6(1)	S(2)–W(2)–P(2)	158.7(2)	P(1)–C–P(2)	97.1(9)
S(1)–W(1)–C(1)	173.9(7)	S(2)–W(2)–C(5)	97.0(5)	W(1)–C(1)–O(1)	171(3)
S(1)–W(1)–C(2)	84.2(6)	S(2)–W(2)–C(6)	82.9(5)	W(1)–C(2)–O(2)	177(2)
S(1)–W(1)–C(3)	92.1(7)	P(1)–W(2)–P(2)	67.8(1)	W(1)–C(3)–O(3)	176(3)
S(1)–W(1)–C(4)	87.7(7)	P(1)–W(2)–C(5)	91.2(5)	W(1)–C(4)–O(4)	173(2)
S(2)–W(1)–C(1)	83.1(7)	P(1)–W(2)–C(6)	86.0(5)	W(2)–C(5)–O(5)	174(1)
S(2)–W(1)–C(2)	173.1(5)	P(2)–W(2)–C(5)	85.3(5)	W(2)–C(6)–O(6)	176(2)
S(2)–W(1)–C(3)	93.4(7)	P(2)–W(2)–C(6)	93.9(5)	S(1)–C(11)–C(12)	116(1)
S(2)–W(1)–C(4)	91.3(6)	C(5)–W(2)–C(6)	177.2(8)	S(1)–C(11)–C(16)	125(1)
C(1)–W(1)–C(2)	90.1(8)	W(1)–S(1)–W(2)	74.0(1)	S(2)–C(21)–C(22)	122(1)
C(1)–W(1)–C(3)	89.7(9)	W(1)–S(1)–C(11)	107.7(7)	S(2)–C(21)–C(26)	118(1)
C(1)–W(1)–C(4)	90.1(9)	W(2)–S(1)–C(11)	119.6(6)	P(1)–C(31)–C(32)	120(1)
C(2)–W(1)–C(3)	85.7(8)	W(1)–S(2)–W(2)	73.8(1)	P(1)–C(31)–C(36)	119(1)
C(2)–W(1)–C(4)	89.6(9)	W(1)–S(2)–C(21)	1105.4(5)	P(1)–C(41)–C(42)	121(1)
C(3)–W(1)–C(4)	175.2(8)	W(2)–S(2)–C(21)	118.9(7)	P(1)–C(41)–C(46)	1120.1(1)
W(1)–W(2)–S(1)	54.6(2)	W(2)–P(1)–C	97.4(6)	P(2)–C(51)–C(52)	121(1)
W(1)–W(2)–S(2)	56.0(1)	W(2)–P(2)–C(31)	123.6(6)	P(2)–C(51)–C(56)	119(1)
W(1)–W(2)–P(1)	145.9(1)	W(2)–P(1)–C(41)	119.1(6)	P(2)–C(61)–C(62)	120(1)
W(1)–W(2)–P(2)	146.2(2)	C–P(1)–C(31)	102.6(8)	P(2)–C(61)–C(62)	120(1)
W(1)–W(2)–C(5)	93.4(5)	C–P(1)–C(41)	108(1)		
W(1)–W(2)–C(6)	88.8(6)	C(31)–P(1)–C(41)	103.6(8)		

carbonyls (> 0 and $< +1$) in complex **4**. Apparently, there is a W(1) $\rightarrow$ W(2) charge transfer in **4** because of the introduction of the DPPM ligand. In contrast to bridge-forming substitution mode **C**, the unsymmetrical substitution mode **D** leads to slight expansion of the M$_2$S$_2$ core by ca. 0.05 Å of M–M, ca. 0.02 Å of M–S bond distances and ca. 0.35° of MSM angle.

It is worth pointing out that the carbonyls of Mo(CO)$_4$-unit in **3** and W(CO)$_4$ in **4** seem to be further substituted by ligands because the Mo(CO)$_4$-unit in **3** and the W(CO)$_4$-unit in **4** are very similar to that in parent compounds, [Mo$_2$(SPh)$_2$(CO)$_8$] and [W$_2$(SPh)$_2$-(CO)$_8$] (**1**), respectively, but neither [Mo$_2$(SPh)$_2$-(CO)$_4$(S$_2$CNEt$_2$)$_2$]$^{2-}$ and [W$_2$(SPh)$_2$(CO)$_4$(DPPM)$_2$] nor other metal carbonyl-thiolates with multi-S$_2$CNEt$_2$ or DPPM ligands have been isolated even if an excess
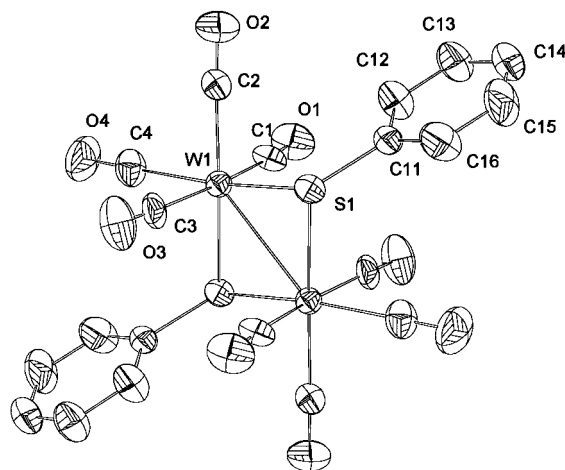
Fig. 1. The structure of [W$_2$(SPh)$_2$(CO)$_8$] (**1**).
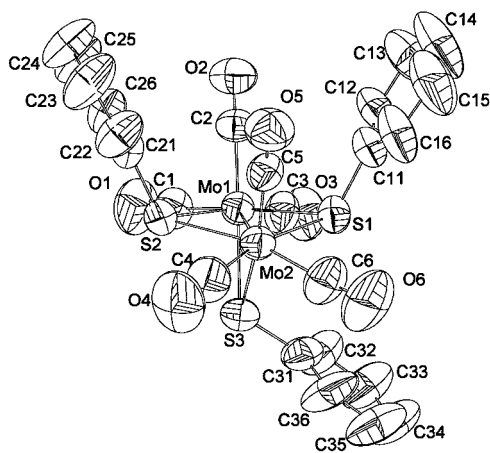
Fig. 2. The structure of the anion 0f [Et₄N][Mo₂(SPh)₃(CO)₆] (**2**).
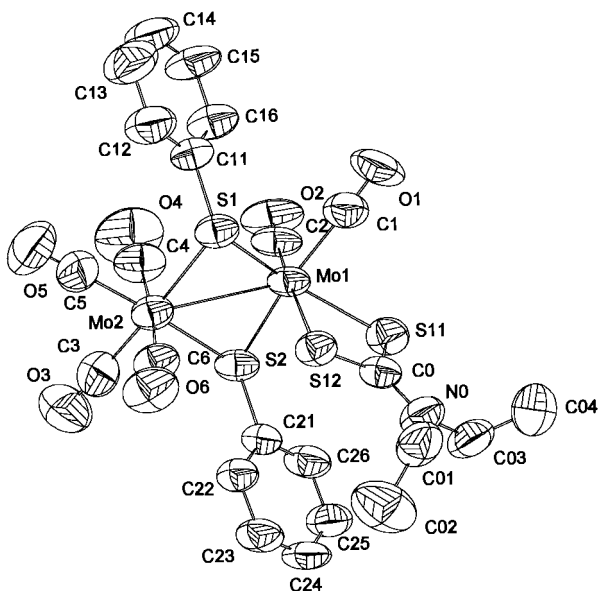
Fig. 3. The structure of the anion of [Bu₄N][Mo₂(SPh)₂(CO)₆-(S₂CNEt₂)] (**3**).

ligands were used in the reaction. This is obviously due to the decreasing stability of the product with multi-ligand and and less of carbonyls.

According to the elemental analysis data of **5** and the similarity of the IR spectra of **5** and a *trans*-substitution mode **A** product, $[M_2(SPh)_2(CO)_6(PPh_3)_2]$ (v_{CO}, 2010(m), 1980(s), 1940(s) and 1905(s) cm^{-1}) [4] in which the P atoms of PPh₃ ligands coordinate to two M atoms, the compound **5** could be assumed as a polymer $[(OC)_3W(SPh)_2W(CO)_3DPPM]_m$ in which the two phosphor atoms of DPPM coordinated to two W atoms in two different $[(OC)_3W(SPh)_2W(CO)_3]$ units forming an infinite chain product although the structure of **5** has not been determined because of its lesser solubility and difficulty to obtain good quality of crystal.

3.3. IR, NMR and cyclic voltammetry

The selected IR data of complexes **1**–**5** are listed in Table 7. It is easy to find that the v_{MC-O} in substituted complexes **2**, **3**, **4** and **5** are lower than that in parent complexes **1** and $[Mo_2(SPh)_2(CO)_8]$, and v_{M-S} of the ligand substituted complexes are higher than that of parent complexes. The lower v_{MC-O} of 1799 and 1840 cm^{-1} in complexes **3** and **4**, respectively are found in the M(0)-compounds $[Mo_2(SPh)_2(CO)_8]^{2-}$ and $[W_2(SPh)_2(CO)_8]^{2-}$ (1770–1790) [1,3,17,18] indicating the existence of a metal-carbonyl unit similar to $M^0(CO)_4$-unit. In fact, the X-ray crystal structure showed that the Mo(CO)₄- and W(CO)₄-units in **3** and **4**, respectively, are similar to that in $[Mo_2(SPh)_2(CO)_8]^{2-}$ [3] and $[W_2(SPh)_2(CO)_8]^{2-}$ [17].

The ^{1}H- and ^{13}C-NMR of the ligand substituted complexes have been measured and focused on the benzene rings (Table 8). The ^{1}H- and ^{13}C-NMR of the PhS ligands in ligand-substituted complexes are observed at 7.14–7.76 and 125.7–148.3 ppm, respectively, which are similar to that in the parent complex **1** and $[Mo_2(SPh)_2(CO)_8]$. Complex **2** contains two sets of $\delta(^1H)$ and $\delta(^{13}C)$ indicating two kinds of Ph-groups in different environment. This is consistent with the result from the X-ray crystal structural data of **2**.

Inspecting the ^{95}Mo-NMR, it can be found that there are two $\delta(^{95}Mo)$ for complex **3**. This implies that complex **3** exists with two kinds of Mo atoms in different coordination environment and oxidation states.

The cyclic voltammograms of **1**, **2**, **3** and **4** are showed in Fig. 5 and the selected CV data are listed in Table 9. As is reported before, complex **1** and $[Mo_2(SPh)_2(CO)_8]$ underwent reversible two-electron reduction at -0.35 V vs SCE ($-0.4/-0.3$ V vs SCE) [1,12] and the current parameter $(I_{Pa}/v^{i/2}AC)$ of complex **1** and $[Mo_2(SPh)_2(CO)_8]$ are 1475 and 1240 A cm $s^{1/2}$ $v^{-i/2}$ mol^{-1}, respectively, (Fig. 5a and b, Table 9). Their electrochemical reaction could be described as following Eq. (a):

$$[M_2(SPh)_2(CO)_8]^0 \underset{-0.40 \text{ V}}{\overset{2e^-}{\rightleftharpoons}} [M_2(SPh)_2(CO)_8]^{2-}$$

$$(M = M, \ W) \tag{a}$$
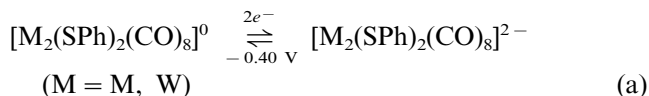
As is shown in Fig. 5c, the complex **2** underwent a reversible reduction at $-0.818(-0.865/-0.770)$ V vs SCE, with $I_{Pc}/I_{Pa} \approx 1$. Its current parameter $(I_{Pa}/v^{1/2}AC)$ of 1121 A cm $s^{1/2}$ $v^{-1/2}$ mol^{-1} is about twice as much as that of ferrocene (688 A cm $s^{1/2}$ $v^{-1/2}$ mol^{-1}obtained in identical conditions). Ferrocene is known to undergo one-electron redox, thus, complex **2** should undergo reversible two-electron reduction at -0.818 V as described in following Eq. (b):

$$[Mo_2(SPh)_3(CO)_6]^- \underset{-0.865 \text{ V}}{\overset{2e^-}{\rightleftharpoons}} [Mo_2(SPh)_3(CO)_6]^{3-} \tag{b}$$
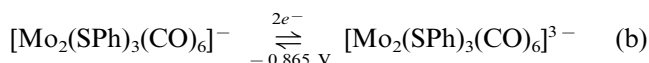
The electrochemical behavior of complex **2** is consistent with that of $[Mo_2(SPh)_2(CO)_6(MeCN)_2]$ (0.8 V vs. SCE), which is a substitution mode **A** product.

The cyclic voltammogram of complex **4**, as shown in Fig. 5d, contained two redox couples at -0.383 and -0.747 V vs SCE with $I_{Pc}/I_{Pa} \approx 1$ and their current parameters are 551 and 531 A cm $s^{1/2}$ $v^{-1/2}$ mol^{-1}. This means that complex **4** undergoes quasi-reversible one-electron redox at -0.383 and -0.747 V vs SCE. This behavior could be expressed as following Eq. (c):

$$[W_2(SPh)_2(CO)_6DPPM]^0$$
$$\underset{-0.383\ V}{\overset{e^-}{\rightleftharpoons}} \{W_2(SPh)_2(CO)_6DPPM\}^-$$
$$\underset{-0.747\ V}{\overset{e^-}{\rightleftharpoons}} [W_2(SPh)_2(CO)_6DPPM]^{2-} \qquad (c)$$
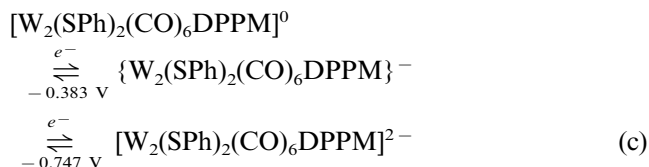
According to the fact that the complex **4** contains two W atoms in different coordination environment: a lower valence tungsten atom (W^L) in $W(CO)_4$-unit and a higher valence tungsten atom (W^H) in $W(CO)_2(DPPM)$-unit ($0 < L < +1$ and $+1 < H < +$
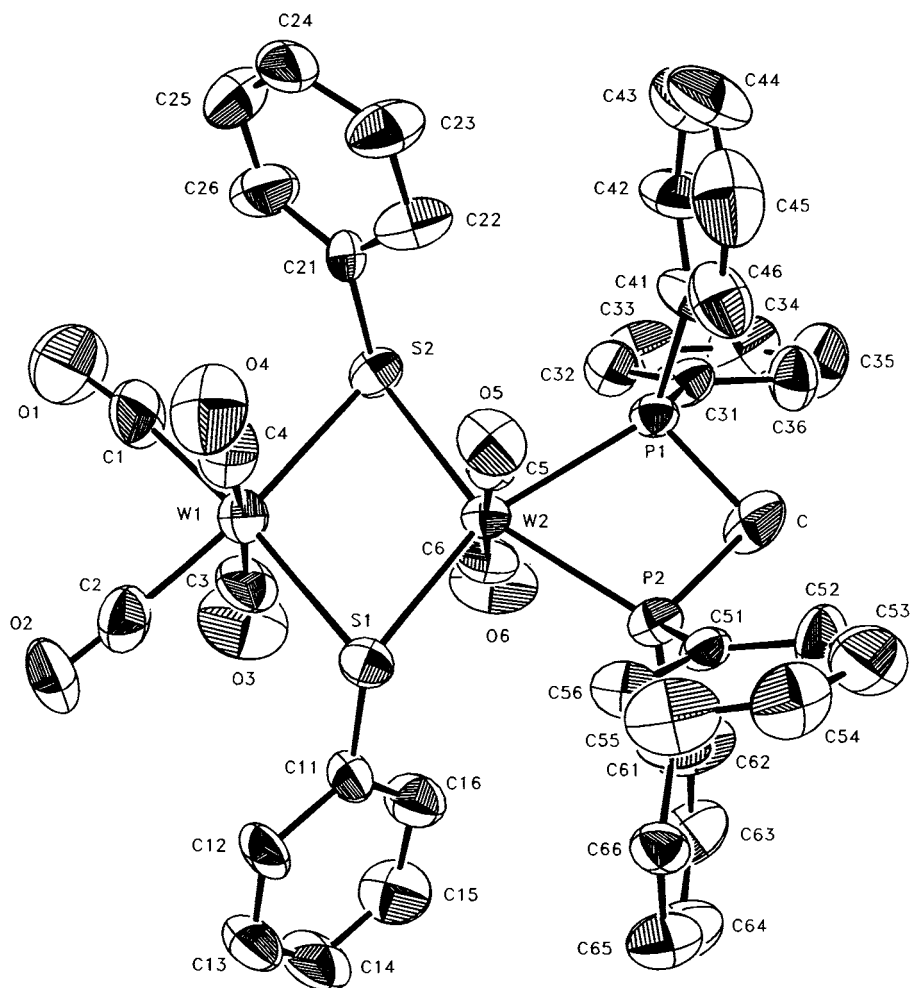
Fig. 4. The structure of $[W_2(SPh)_2(CO)_6DPPM]$ (**4**).

Table 6
Structural parameters of M_2S_2 units in **1**, **2**, **3** and **4**, and arrangement of the Ph rings relative to the M_2S_2–unit plane

Complexes	**1**	**2**	**3**	**4**	$[Mo_2(SPh)_2(CO)_8]$
M–S (Å)	2.47	2.46	2.55, 2.41	2.55, 2.43	2.47
M–M (Å)	2.969	2.877	3.039	2.996	2.962
MSM (°)	73.7	71.38	74.25	74.0	73.56
Arrangement of the Ph rings	*anti-*	*syn-*	*anti-*	*anti-*	*anti-*
M–C (axial) (Å)	2.06, 2.03	1.93, 1.91	1.92, 2.02	2.03, 2.01	2.05, 2.05
M–C (equatorial) (Å)	2.02, 2.00	1.96, 1.97	1.99, 1.96	1.98, 1.97	2.00, 2.04
C–O (Å)	1.135	1.160	1.150	1.145	1.138

Table 7
Selected IR data of **1**, **2**, **3**, **4**, **5** and parent [$Mo_2(SPh)_2(CO)_8$]

Complexes	ν_{MC-O}	δ_{M-C-O}	ν_{M-C}	ν_{M-S}
1	2031s	569m	357m	426m
	1963s	557m	339m	407m
	1939s	488m		
		459m		
2	1998m			
	1965s	608m	370w	433sh
	1940s	579m	351m	419m
	1917s	507m		
	1849s	498m		
3	2017s	507m	372m	447m
	1928s	500m	361m	436m
	1898s	476m	345w	
	1799s			
4	2033m	598m	357m	428m
	1956s	575m	339w	409m
	1925s	559m	318w	374m
	1840m			
5	2006w	598m	–	426m
	1979s	581mm		413m
	1927s	548m		
	1896s			
[$Mo_2(SPh)_2(CO)_8$]	2065sh			
	2030s	567/560s	353m	421w
	1994s	551s	338m	407m
	1975s	488m		382m
	1947s	459wm		

2), it is reasonable to speculate that the different redox event occurs on the different W metal centers. When the scan goes to negative potential the one-electron reduction, at first, occurs on the higher valence W^H center, at -0.383 V, and then occurs on the lower valence W^L center at -0.747 V.

Inspecting the changes of CV behavior for ligand substituted complexes with different substitution modes it is clear to be found that the two-electron transfer character of the complexes [$M_2(SPh)_2(CO)_8$]$^{2-,0}$ (M = Mo, W) is not only dependent upon the planarity but also the symmetry of the M_2S_2-unit in the complexes.

Complex **2** still keeps the two-electron transfer character because of its remaining the planarity and symmetry of the Mo_2S_2-unit. Complex **4** no longer possesses two-electron transfer character for its planar W_2S_2-unit lost symmetry. Complex **3** exhibited somewhat more complicated CV behavior implying some decomposition of the sample. However, obviously, complex **3** does not possess two-electron transfer character because of the same reason as complex **4**.

4. Summary

Four new dinuclear M(I) complexes (M = Mo or W), [$W_2(SPh)_2(CO)_8$] (**1**), [$Mo_2(SPh)_3(CO)_6$]$^-$ (**2**), [$Mo_2(SPh)_2(CO)_6(S_2CNEt_2)$]$^-$ (**3**) and [$W_2(SPh)_2(CO)_6(DPPM)$] (**4**) and a polymer [$W_2(SPh)_2(CO)_6(DPPM)$]$_m$ (**5**) were synthesized by the reaction of [$M_2(SPh)_2(CO)_8$] (M = Mo, W) with appropriate ligands and reaction conditions. The complexes were studied by crystal structure determination, IR, NMR and CV measurement. Three ligand substitution modes (*trans*-substitution mode **A**, bridge-forming substitution mode **C** and unsymmetrical substitution mode **D**) and two kinds of planar M_2S_2-units (symmetrical and unsymmetrical) were found in the complexes. Modes **A** and **C** make the complexes possess two-electron transfer character and mode **D** leads to formation of mixed valence metal atoms and lose of two-electron transfer character.

5. Supplementary material

Crystallographic data for the structural analysis have been deposited with the Cambridge Crystallographic Data Centre, CCDC no. 165472, 165471, 165583 and 165470 for compounds **1**, **2**, **3** and **4**, respectively. Copies of this information may be obtained free of charge from The Director, CCDC, 12, Union Road, Cambridge CB2 1EZ (Fax: + 44-1223-336033; e-mail: deposit@ccdc.cam.ac.uk or www: http://www.ccdc.cam.ac.uk).

Table 8
Selected ^{1}H-, ^{13}C- and ^{95}Mo-NMR data of **1**, **2**, **3** and [$Mo_2(SPh)_2(CO)_8$] (ppm)

Complexes	δ ^{1}H (Ph)			δ ^{13}C (Ph)			δ ^{95}Mo
	o–H	m–H	p–H	o–C	m–C	p–C	
2	7.46	7.20	7.18	135.5	128.8	125.9	-853.7
	7.55	7.38	7.30	130.0	128.0	124.7	
3	7.14–7.76			148.3–125.7			-1487.9
1	7.26–7.55			142.5–128.0			–
[$Mo_2(SPh)_2(CO)_8$]	7.25–7.51			142.5–128.0			-1110.3
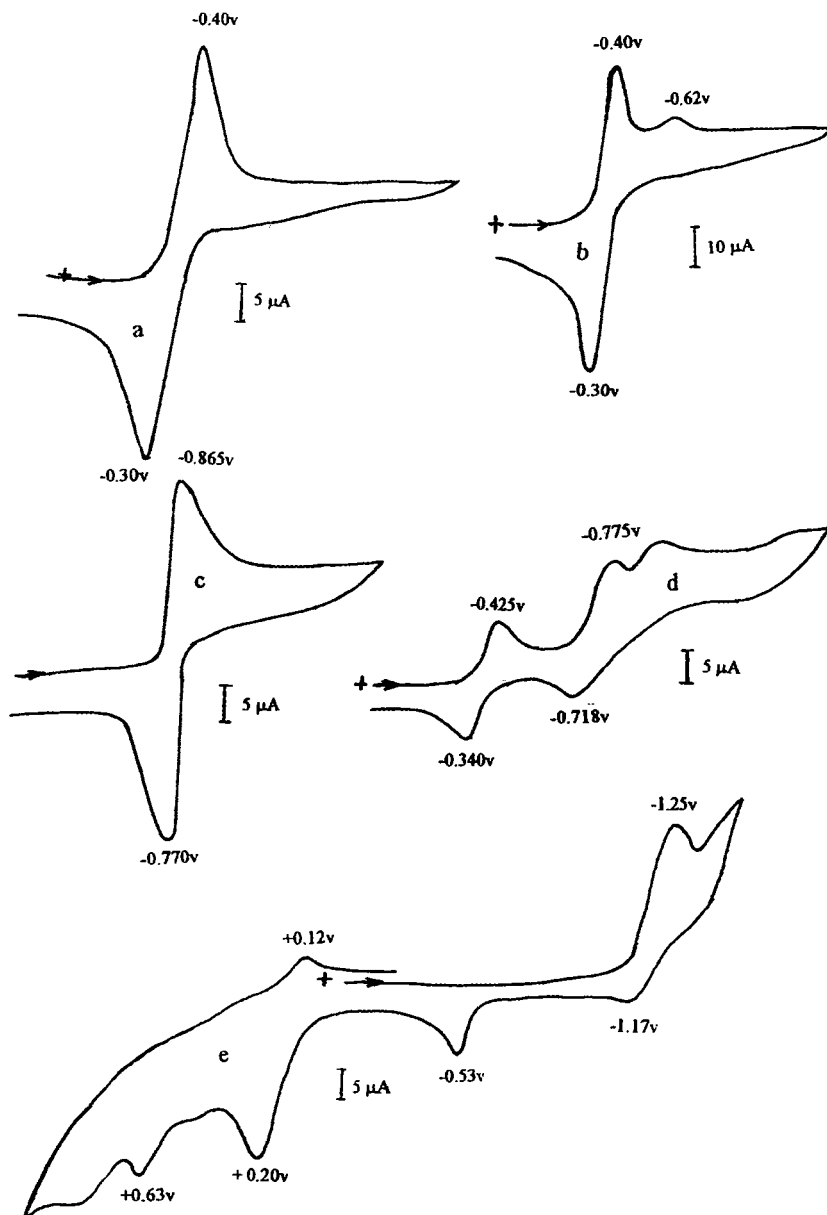
Fig. 5. The voltammograms of **1**, **2**, **3**, **4** and [Mo$_2$(SPh)$_2$(CO)$_6$]. (a) **1** in Me$_2$CO, v, 100 mv s^{-1}, sample concentration, 0.001 M; (b) [Mo$_2$(SPh)$_2$(CO)$_6$] in Me$_2$CO, v, 100 mv s^{-1}, sample concentration, 0.001 M; (c) **2** in Me$_2$CO, v, 100 mv s^{-1}, sample concentration, 0.001 M; (d) **4** in Me$_2$CO, v, 100 mv s^{-1}, sample concentration, 0.001 M; (e) **3** in Me$_2$CO, v, 100 mv s^{-1}, sample concentration, 0.001 M.

Table 9
CV data of **1**, **2**, **3**, **4** and [Mo$_2$(SPh)$_2$(CO)$_8$] (V vs. SCE)

Complexes	E_C	E_a	$E_{1/2}$	i_{Pc}/i_{Pa}	$I_{Pa}/v^{1/2}AC$
1	−0.40	−0.30	−0.35	0.962	1475
2	−0.865	−0.770	−0.818	0.983	1121
4	−0.425	−0.340	−0.383	0.892	551
	−0.775	−0.718	−0.747	0.926	531
3	−1.25	−1.17	−1.21		
		−0.53	−0.53		
	+0.12	+0.20	+0.16		
	+0.63		+0.63		
[Mo$_2$(SPh)$_2$(CO)$_8$]	−0.40	−0.30	−0.35	0.900	1240

Acknowledgements

References

[1] B. Zhuang, J.W. McDonald, F.A. Schultz, W.E. Newton, Organometallics 3 (1984) 943.

[2] D.A. Smith, B. Zhuang, W.E. Newton, J.W. McDonald, F.A. Schultz, Inorg. Chem. 26 (1987) 2524.

[3] B. Zhuang, L. Huang, L. He, Y. Yang, J. Lu, Inorg. Chim. Acta 157 (1989) 85.

[4] (a) B. Zhuang, L. Huang, L. He, Y. Yang, J. Lu, Acta Chim. Sinica 47 (1989) 25;
(b) Inorg. Chim. Acta 127 (1987) L7.

[5] G. Pan, B. Zhuang, J.-T. Chen, Acta Cryst. C54 (1998) 1580.

[6] G. Pan, B. Zhuang, J.-T. Chen, Acta Cryst. C55 (1999) 298.

[7] G. Pan, B. Zhuang, L. He, J. Chen, J. Lu, Chem. Lett. (1998) 1103.

[8] G. Pan, B. Zhuang, J.-T. Chen, Acta Cryst. C54 (1998) 1815.

[9] G. Pan, B. Zhuang, J.-T. Chen, Acta Cryst. C55 (1999) 297.

[10] G. Pan, B. Zhuang, L. He, J.-T. Chen, J. Chen, J. Lu, J. Organomet. Chem. 580 (1999) 313.

[11] B. Zhuang, L. Huang, L. He, Chin. J. Struct. Chem. 14 (1995) 359.

[12] B. Zhuang, J.W. McDonald, F.A. Schultz, W.E. Newton, Inorg. Chim. Acta 99 (1985) L29.

[13] R.C.G. Killean, J.L. Lawrence, Acta Cryst. 25 (1969) 1750 Sect. B.

[14] MoLEN, An Interactive Structure Solution Procedure, Enraf-Nonius, Delft, The Netherlands, 1990.

[15] G.M. Shedrick, SHELXTL Version 5.03, Siemens Analytical X-ray Instrument Inc., Madison, WI, 1990.

[16] H. Sun, B. Zhuang, L. Huang, L. He, Chin. J. Struct. Chem. 18 (1999) 32.

[17] D.J. Darensbourg, K.M. Sanchez, J. Reibenspies, Inorg. Chem. 27 (1988) 3636.

[18] L. He, B. Zhuang, B. Chen, S. Cai, L. Zhang, Chin. J. Struct. Chem. 16 (1997) 129.